Biochimica et Biophysica Acta, 1111 (1992) 185–196
© 1992 Elsevier Science Publishers B.V. All rights reserved 0005-2736/92/$05.00

BBAMEM 75775

Exchange efflux of [^{3}H]palmitate from human red cell ghosts to bovine serum albumin in buffer. Effects of medium volume and concentration of bovine serum albumin.

Inge N. Bojesen and Eigil Bojesen

Institute of Biochemistry B, University of Copenhagen, Panum Institute, Copenhagen (Denmark)

(Received 24 March 1992)

Key words: Palmitate; Fatty acid transport; Erythrocyte ghost; Unstirred layer; Efflux kinetics

[^{3}H]Palmitate, PA, exchange efflux kinetics is recorded from human erythrocyte ghosts to buffer with bovine serum albumin, BSA, at 0°C. The effects have been investigated of three medium/ghost volume ratios: 36, 80 and 500, of six BSA concentrations, [BSA]: 0.01, 0.02, 0.05, 0.2, 1 and 2% (1.5, 3.0, 7.5, 30, 150 and 300 μM) and of various ν, molar ratios of palmitate to BSA, between 0.15 and 0.94. Data are analyzed in terms of a virtually closed three-compartment model. In theory, the tracer efflux is biexponential and the rate coefficients differ at least 20 fold [1]. The efflux rate at 2% BSA is monoexponential beyond our resolution time of about 1 s, but nearly biexponential at or below 0.2% BSA with a well-defined smallest-rate coefficient β. β depends strongly on [BSA] but is remarkably ν independent. The medium/ghost volume ratio has no effect on β when [BSA] $\geq$ 0.2%, although β measured at 2% BSA is almost 2-fold higher than at 0.2%. This suggests the presence of an unstirred layer, USL. According to our model, the observations are understood quantitatively on basis of our previously published dissociation rate constants of the PA-BSA complex, as well as PA equilibrium bindings to ghost membranes (Bojesen, I.N. and Bojesen, E. (1991) Biochim. Biophys. Acta 1069, 297–307). Essentially, β is theoretically a function of two terms, one comprising the membrane transport parameters and the other the medium-dependent variables. Most important is the clearance with respect to monomer concentration adjacent to the membrane. The clearance is calculated on basis of quasistationary diffusion in USL. The data are compatible with a planar USL of 6 μm depth and with the same area as a ghost but not with a spherical USL.

Introduction

Conventionally, the transfer between serum and cells of long-chain fatty acids (FA) such as palmitate (PA) is mediated by the very low water-phase concentrations of monomers. This concept has been challenged by two quite recent observations [2–4]. Firstly, it was impossible to demonstrate any monomer PA in the dialysate of PA-albumin complexes by using FA permeable artificial membranes [2,3]. Secondly, cellular uptake of FA increases with the concentration of FA-albumin complex, approaching a maximum with the physiological albumin concentration in serum, although ν, the molar ratio of FA to albumin and, therefore, the equilibrium water-phase concentration remains constant [4]. In both studies [2,4], the transfer of FA between serum and cells is explained by direct contact between albumin and cell membranes, suggesting 'albumin receptors' on the cell surface.

The many strong arguments speaking against the 'albumin receptor' notion have been reviewed recently in a report on the albumin effect on the PA efflux from an organic phase [5]. We may add the facts that PA is readily transferred between resealed red cell membranes, ghosts, and buffer with albumin [1], although direct albumin contact with the bilayer is blocked by a 10 nm glycocalyx space [6].

With a new method, not using artificial membranes or organic phases, we have recently reported [7] on the presence of a ν-dependent water-phase concentration of PA in equilibrium with PA bound to cell membranes and/or BSA. Our concentrations with ν 0.5 and 1.0 are about 3-fold lower than those measured by Spector et al. [8,9], using the phase partition method of Goodman [10] and it is interesting that our values were predicted by Spector [11] to be the true monomer concentrations when the most probably theoretical errors of the phase-partition method are taken into consideration.

Correspondence to: I.N. Bojesen, Institute of Biochemistry B, University of Copenhagen, Panum Institute, Blegdamsvej 3C, DK-2200 Copenhagen N, Denmark.

The aim of most work on FA transfer between albumin and cell membranes is to identify the mechanism of the membrane transport because a simple diffusion through the lipid bilayer is unlikely. Compared with FA transport through artificial bilayers [12], the much faster cellular uptake suggests some sort of facilitated diffusion [13–17]. Saturation kinetics of a transport strongly suggests that the transport is mediated by a carrier and such a kinetics has been claimed for FA uptake by some cells [13–17] when the water-phase equilibrium concentration of FA is assumed to represent the effective concentration of the substrate, i.e., the water-phase concentration adjacent to the membrane. However, the dissociation rate of FA from its albumin binding and the transport through an unstirred layer (USL) are necessarily determinants of the mentioned effective substrate concentration, because the initial amount of monomer FA is too small to support any measurable cellular uptake.

The aim of the present work is to obtain information on the determinants of the effective substrate concentration presented to suspended cells. Ghost suspensions are most suitable for studying the transport between the membrane and medium albumin because FA are not metabolized and tracer exchange transport is, therefore, feasible. This technique greatly facilitates unequivocal data analysis.

Previous work [1] confirmed another observation [18] that erythrocyte membranes have a considerable FA binding capacity. We showed that bound PA is mainly located at the inner surface of the membrane and the kinetic model of the transport to the medium was confirmed in exchange efflux experiments with ghosts containing BSA. The latter experiments revealed for the first time that PA transport is mediated by a binding capacity and that the dissociation rate constant of PA-BSA complex increases with ν. These observations are all used in the present work. The [BSA] was in our previous work always 0.2% and the work of Weisiger et al. [5] suggested to us that ghost suspensions could be an ideal tool to get information of the albumin effect on FA transport into and out of cells in suspensions, in terms of USL.

The physical basis of USL around suspended cells is different from that above a superflushed planar large surface as described by Weisiger et al. [5], in which case the value is about 50 μm. For suspended cells, the depth of USL depends not only on the stirring efficiency, the cell density and the density ratio of cells to medium but also on the diffusion coefficient of the solute [19]. Furthermore, the geometry of USL around suspended cells is unknown, but it is mostly assumed to be planar which means that we are dealing with diffusion in one dimension [20,21]. It is not yet possible to predict the depth of USL but we can find the characteristics of USL, which fit a variety of data. This requires a considerable theoretical section because only the basic idea of the related previous work [5] is applicable to our experiments. The reason is that the theory does not account for the contribution of tracer uptake in the stirred volume fraction, which in some situations may be just as important as that in the USL of suspended cells when the depth of USL is only a few μm [20]. The problem is solved by applying the principle of independent diffusion streams [22]. Furthermore, a narrow USL implies that it is possible to apply the compartmental model because the diffusion of bound tracer is then an unimportant rate determinant as demonstrated in the Appendix.

An important implementation is that, in order to investigate the transport kinetics, cellular uptake is to be related to the effective monomer concentration, whereas the monomer equilibrium concentration is irrelevant.

Materials and Methods

Materials

[9,10-^{3}H]Palmitic acid (spec. act. 1.91 TBq/mmol) was obtained from Amersham, Amersham, UK. Unlabelled palmitic acid was obtained from Sigma. Tracer palmitic acid was purified every six months by chromatography on a Daltosil 75 (Serva) column using 0.05% acetic acid and 0.05% ethyl acetate in benzene as eluant.

Bovine serum albumin (BSA) (Behring Institute, Germany) was defatted according to the method of Chen [23].

Experiments with the medium/ghost volume ratio, V_ω, 500 and 80 (see methods) were carried out in a thermostatic controlled vessel (44 mm × 37 mm i.d.) with a 25 mm TRIKA stirring bar (Janke and Kunkel, Germany) and the V_ω-36 experiments in a smaller conical vessel (44 mm × bottom to edge 15–30 mm i.d.) with an egg-shaped stirring bar (19 × 9.5 mm).

Methods

The technique for preparing a uniform population of resealed 'pink' ghosts from human erythrocytes is described in detail previously [1]. The ghosts are all prepared without intracellular BSA and stored in 0.01% BSA in 165 mM KCl, 2 mM phosphate buffer (pH 7.3) at 4°C until efflux experiments were performed. The preparation of media (charge buffers) for labelling of the ghosts with [^{3}H]palmitic acid was done with the glass bead technique [24]. The radioactive ghosts were separated from the charge buffer by centrifugation 5 min at 0°C at 22 200 rpm (36 500 × g) and washed twice with 10 volume of 165 mM KCl, 2 mM phosphate buffer at 0°C. These washed suspended ghosts were distributed onto 80 mm plastic tubes (i.d. 3 mm) and packed by centrifugation 15 min at 50 000 × g and 0°C.

300 μl packed ghosts containing 20% extracellular buffer were injected into 9 ml or 20 ml stirred isotope-free 165 mM KCl, 2 mM phosphate medium 0°C (pH 7.3), containing different percentages of BSA and unlabelled palmitate (called V_Θ-36 or V_Θ-80 experiments, respectively). In V_Θ-500 experiments, 80 μl packed ghosts was injected into 33 ml efflux buffer. Serial sampling of ghost-free efflux medium was done with the Millipore-Swinnex filtration technique as described previously [1]. Radioactivity of filtrates was measured by counting duplicates of 400 μl in 3.9 ml Opti-fluor scintillation fluid to a probable error smaller than 1.5% and less than 5% for the initial samples. We have not estimated directly the precision by which time periods of incubations are recorded, but our data on the initial efflux indicate about 0.5 s.

Statistics and data analyses

We have used the methods described by Armitage [25] to calculate the statistics, weighted means and probabilities of significance of differences.

The Hewlett Packard 85 B PC is used extensively: as a sampling timer, to tape the timing and counting rates, to calculate and plot the efflux data and to estimate regression lines of $-\ln(1-y/y_\infty)$ vs. time including the errors on the estimates of slope and ordinate intercept. At high [BSA], our resolution time (about 1 s) does not allow sufficient data to be provided on the initial tracer release. Therefore, fits with the expected biexponential time-course cannot be assessed.

At 0.2% or lower [BSA], the plots show a decreasing slope (see Fig. 2) and the regression is calculated for the linear final part from which we usually exclude points with ordinate values above 2.5, because the uncertainty of ordinate values is rapidly increasing as y/y_∞ approaches 1.

Theory

Notations

A,	the concentration of bound PA
P,	the water-phase concentration of PA equal to $\nu/(K_a\,(3-\nu))$.
ν,	the molar ratio of PA to BSA $=A/$[BSA]
k_1:	the ν-dependent dissociation rate constant of PA-BSA complex at 0°C [1]
K_a:	the apparent equilibrium constant ($2.3\cdot10^8$ M^{-1}) of PA binding to BSA at 0°C, calculated for three binding sites and $\nu \leq 1.5$ [7]
k_3, k_5,	rate constants defined in Fig. 1
k_a,	the first-order rate constant of binding the monomer palmitate to BSA, equal to $K_a\cdot k_1$ [BSA] $(3-\nu)=k_1\,A/P$
V_Θ,	volume of the medium (ml or 10^{12} μm^3) referred to 1 ml ghosts (approx. $9\cdot10^9$ ghosts)
V_u,	volume of unstirred medium (unit as V_Θ)
V_s,	$(V_\Theta - V_u)$ volume of stirred medium (unit as above)
S,	surface area of ghosts (μm^2). (Mean ghost area 144 μm^2 [1])
δ,	depth of V_u, δ in μm is obtained as $V_u\cdot10^{12}/(9\cdot10^9\cdot144)=V_u/1.3$
D,	diffusion coefficient of PA in water at 0°C (360 μm^2 s^{-1})[26]
y,	tracer efflux at any time t (dpm)
y_∞,	tracer efflux at infinite time (dpm)
y/y_∞,	the fractional tracer efflux
Cl,	'clearance' (ml/s), a water-phase volume normalized to 1 ml ghost, which in steady-states contains the amount of tracer monomer bound to BSA per s in any compartment
cl,	the corresponding 'clearance' (μm^3/s) normalized to one ghost
R_D,	diffusion resistance in the unstirred volume surrounding 1 ghost (s/μm^3)

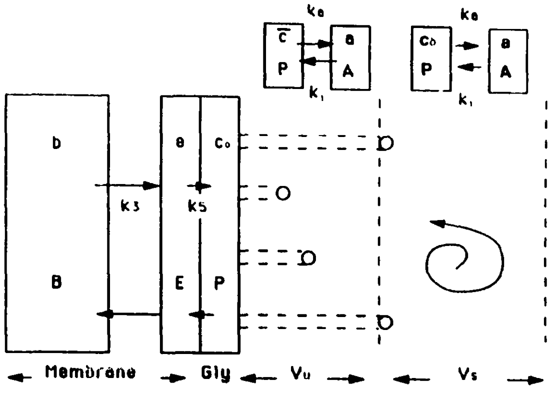

Fig. 1. In ghosts membranes, PA is bound in a large inner pool, spec. act. b/B and in a smaller outer pool, spec. act. e/E. k_1 is the dissociation rate constant of PA-BSA complex. k_3 is the rate constant of unidirectional flow in direction B to E. k_5 is the rate constant of unidirectional flow from E to the monomer pool of a 10 nm deep glycocalyx space. The specific activity is in this space c_0/P. c/P is the specific activity of monomer in the unstirred volume V_u, depth δ μm. c/P is a function of r, between r_0 and δ. The integrated mean value is $\bar{c}/P$. The uptake of monomer on BSA in V_u and V_s is determined by a first-order rate constant (k_a, which is a function of [BSA] and of ν) and generates the monomer diffusion streams in V_u represented by ===○. The specific activity of PA on BSA (a/A) is independent of r. The specific activity of monomer in the stirred volume V_s is everywhere c_δ/P. V_s communicates with the glycocalyx space only by diffusion in V_u.

1. Quasistationary diffusion of the dissolved monomer tracer in V_u with BSA

The uptake on BSA of PA generates a diffusion gradient of monomer tracer concentration, c, in V_u so that diffusion is anywhere matched by net uptake on BSA. Our results are incompatible with a diffusion in three dimensions (spherical geometry of unstirred layer, see Discussion) whereas they fit diffusion in one dimension. The net uptake at any distance from the ghost surface (r) is the product of the unidirectional PA release rate (k_1 A) and the difference in specific activities ($c/P - a/A$). The differential equation which expresses that the supply by diffusion is equal to this net uptake is:

$$D(\mathrm{d}^2c/\mathrm{d}r^2) = k_1A(c/P - a/A)$$

where a is the concentration of bound tracer assumed to be independent of r and uniform in the whole medium. Our arguments for this assumption, essentially based upon the small depth of the diffusion layer, are presented in the Appendix.

The transform

$$\mathrm{d}^2c/\mathrm{d}r^2 - \lambda^2c = -k_1a/D, \quad \lambda = \sqrt{(k_1A/P)/D}$$

has the general solution

$$c = aP/A + \alpha\sinh(\lambda r) + \beta\cosh(\lambda r) \tag{1}$$

where α and β are the two integration constants.

General boundary conditions for ghosts in a large unstirred volume:
(1) at $r \to \infty$, then $c_\infty \to aP/A$ and $\sinh(\lambda r) \to \cosh(\lambda r)$, thus, $\beta = -\alpha$
(2) at $r = 0$, $c_0 = aP/A - \alpha$, therefore,

$$c = \frac{aP}{A} + (c_0 - aP/A)\mathrm{e}^{-\lambda r} \tag{2}$$

We now want to calculate the mean value of c, $\bar{c}$, within the limited volume of diffusion, $S\delta$, this is

$$\bar{c} = \frac{S}{S\delta}\int_0^\delta c\,\mathrm{d}r$$

or

$$\bar{c} = \frac{aP}{A} + \frac{aP/A - c_0}{\delta}\left(\frac{\mathrm{e}^{-\lambda\delta} - 1}{\lambda}\right) \tag{2.1}$$

Introducing $u \cdot c_0 = \bar{c}S\delta$ gives

$$u = \frac{aPS\delta}{Ac_0} + S\left(1 - \frac{aP}{AC_0}\right)\left(\frac{1 - \mathrm{e}^{-\lambda\delta}}{\lambda}\right)$$

or

$$u = u_\mathrm{i}\left(1 + \frac{a/A}{c_0/P}\left(\frac{S\delta}{u_\mathrm{i}} - 1\right)\right) \tag{3}$$

where $u_\mathrm{i} = S((1 - \mathrm{e}^{-\lambda\delta})/\lambda)$ μm^3 per ghost when $(aP)/(Ac_0)$ is approx. 0 for low values of y/y_∞, u is equal to u_i. u_i is defined by λ, δ and S. When we want to express u and u_i in terms of ml per ml ghosts, we divide by the conversion factor 111 ($10^{12}/(9 \cdot 10^9)$ μm^3 per ghost) and use upper-case letters.

II. Definition of Cl_u, Cl_s and Cl_Σ

The theory on the combined effects on c_0 of tracer uptake by BSA in V_u and V_s

The net uptake of tracer (F1) in v_u can be expressed as:

$$\mathrm{F1} = v_\mathrm{u}k_1A(\bar{c}/P - a/A) = v_\mathrm{u}k_a(\bar{c} - aP/A)$$

using $\bar{c}$ given by Eqn. 2.1 and u_i given by the expression

$$u_\mathrm{i} = S((1 - \mathrm{e}^{-\lambda\delta})/\lambda) \text{ (see above)}$$

we get

$$\mathrm{F1} = v_u k_a(c_0 - aP/A)\mathrm{u_i}/(\delta S)$$

and, since $\delta S = v_\mathrm{u}$

$$\mathrm{F1} = k_a u_\mathrm{i}(c_0 - aP/A) = \mathrm{cl}_\mathrm{u}(c_0 - aP/A)$$

F2, the net uptake of tracer in v_s is analogous to F1:

$$\mathrm{F2} = v_\mathrm{s}k_a(c_\delta - aP/A) = \mathrm{cl}_\mathrm{s}(c_\delta - aP/A)$$

Thus, clearance is analogous to conductivity.

We can further apply the concepts of Ohm's law by analogy with formally similar problems in heat conduction.

The current (F2) in v_u is the potential difference ($c_0 - c_\delta$) divided by the resistance R_D, whereby we get $\mathrm{F2} = (c_0 - c_\delta)/R_\mathrm{D}$, eliminating c_δ from the two expressions of F2 gives

$$\mathrm{F2} = (c_0 - aP/A)/(R_\mathrm{D} + 1/\mathrm{cl}_\mathrm{s})$$

The quasistationary efflux of tracer (F = F1 + F2) is based upon the principle of independent diffusion streams advocated by Jacobs [22].

The total flow from c_0 to the two binding capacities (BSA in v_u and v_s) are then simply

$$\mathrm{F} = \mathrm{F1} + \mathrm{F2} = (c_0 - aP/A)(\mathrm{cl}_\mathrm{u} + \mathrm{cl}_\mathrm{s}/(1 + \mathrm{cl}_\mathrm{s}R_\mathrm{D})) = (c_0 - aP/A)\mathrm{cl}_\Sigma$$

when $\mathrm{cl}_\Sigma = \mathrm{cl}_\mathrm{u} + \mathrm{cl}_\mathrm{s}/(1 + \mathrm{cl}_\mathrm{s}R_\mathrm{D})$ or normalized to 1 ml ghost $\mathrm{Cl}_\Sigma = \mathrm{Cl}_\mathrm{u} + \mathrm{Cl}_\mathrm{s}/(1 + \mathrm{cl}_\mathrm{s}R_\mathrm{D})$, when R_D is calculated for one ghost.

R_D. The diffusion resistance of V_u

The diffusion resistance of a plane sheet with the area $S = 4\pi r^2$ and thickness δ is according to Crank (Eqn. 4.4 [27]) $R_\mathrm{D} = \delta/(4\pi r^2\ \mathrm{D})$. In contrast, the diffusion resistance of a shell, depth δ', surrounding a sphere with radius r is $R_\mathrm{D} = \delta'/(4\pi r(r + \delta')D)$ according to Crank (Eqn. 6.7 [27]).

III. The rate constant of [^{3}H]palmitate exchange efflux

Using the signature of Fig. 1, we can write

$$-\mathrm{d}b/\mathrm{d}t = k_3B(b/B - e/E) = k_3b - k_3eB/E \qquad (4)$$

and, when y is the tracer of the medium volume per ml ghosts

$$\mathrm{d}y/\mathrm{d}t = k_5E(e/E - c_0/P) \qquad (4.1)$$

Moreover, the net flux $\mathrm{d}y/\mathrm{d}t$ expressed in terms of clearance is $\mathrm{d}y/\mathrm{d}t = \mathrm{Cl}_{\Sigma}(c_0 - aP/A)$, since $a = y/V_{\Theta}$ we can write

$$\mathrm{d}y/\mathrm{d}t = \mathrm{Cl}_{\Sigma}c_0 - \mathrm{Cl}_{\Sigma}Py/(V_{\Theta}A) \qquad (5)$$

eliminating c_0 from Eqns. 4.1 and 5 gives

$$e = \mathrm{d}y/\mathrm{d}t((1/k_5) + (1/\mathrm{Cl}_{\Sigma})E/P) + Ey/(V_{\Theta}A) \qquad (4.2)$$

With T as the tracer dose we have $T = b + e + y$ and, therefore

$$b = T - y - \mathrm{d}y/\mathrm{d}t((1/k_5) + (1/\mathrm{Cl}_{\Sigma})E/P) - Ey/(V_{\Theta}A)$$

Differentiation gives

$$-\mathrm{d}b/\mathrm{d}t = \mathrm{d}y/\mathrm{d}t + \mathrm{d}^2y/\mathrm{d}t^2((1/k_5) + (1/\mathrm{Cl}_{\Sigma})E/P)$$
$$+ E/(V_{\Theta}A)\mathrm{d}y/\mathrm{d}t$$

Using Eqn. 4, we get after rearrangements

$$\frac{\mathrm{d}^2y}{\mathrm{d}t^2} + \left[k_3\left(1 + \frac{B}{E}\right) + \frac{k_5\mathrm{Cl}_{\Sigma}}{\mathrm{Cl}_{\Sigma} + \frac{k_5E}{P}}\left(1 + \frac{E}{V_{\Theta}A}\right)\right]\frac{\mathrm{d}y}{\mathrm{d}t}$$
$$+ \left[\frac{k_3k_5\mathrm{Cl}_{\Sigma}}{\mathrm{Cl}_{\Sigma} + \frac{k_5E}{P}}\left(1 + \frac{E}{V_{\Theta}A} + \frac{B}{V_{\Theta}A}\right)\right]y = T\frac{k_3k_5\mathrm{Cl}_{\Sigma}}{\mathrm{Cl}_{\Sigma} + \frac{k_5E}{P}}$$

with the solution $y = C'1 \cdot \mathrm{e}^{-\alpha t} + C'2\mathrm{e}^{-\beta t} + T/(1 + E/(V_{\Theta}A) + B/(V_{\Theta}A))$ when $C'1$ and $C'2$ are integration constants and α and β are rate coefficients.

Now, $T/y_{\infty} = (V_{\Theta}A + E + B)/(V_{\Theta}A)$ and, therefore, $y = C'1 \cdot \mathrm{e}^{-\alpha t} + C'2 \cdot \mathrm{e}^{-\beta t} + y_{\infty}$ which is correct for $t \rightarrow \infty$. It is convenient to use it in the form

$$(1 - y/y_{\infty}) = C1 \cdot \mathrm{e}^{-\alpha t} + C2 \cdot \mathrm{e}^{-\beta t} \qquad (6)$$

where $C1 = -C'1/y_{\infty}$ and $C2 = -C'2/y_{\infty}$.

The differential equation and its solution Eqn. 6 is similar to the differential equation (and its solution Eqn. 4) used previously [1], but the important difference is that k_5 in the previous paper signifies the rate constant of unidirectional flow from the E compartment to BSA, whereas k_5 now signifies the unidirectional flow from the E compartment to the adjacent water phase.

The rate coefficients α and β are related to the parameters of the system by $\alpha + \beta = k_3(1 + B/E) + (1 + E/(V_{\Theta}A))k_5\mathrm{Cl}_{\Sigma}/(\mathrm{Cl}_{\Sigma} + k_5\ E/P)$ and $\alpha\beta = (1 + E/(V_{\Theta}A) + B/(V_{\Theta}A))k_3k_5\mathrm{Cl}_{\Sigma}/(\mathrm{Cl}_{\Sigma} + k_5E/P)$

From these equations we get

$$\beta = \frac{T/y_{\infty}(1 + \beta/\alpha)}{\frac{E + B}{P\mathrm{Cl}_{\Sigma}} + \frac{1 + \frac{E}{V_{\Theta}A}}{k_3} + \frac{1 + \frac{B}{E}}{k_5}} \qquad (7)$$

β/α in this equation can be evaluated from experiments in which T/y_{∞} and $1 + E/(V_{\Theta}A)$ is approx. 1, that is when $V_{\Theta}A >> E + B$. In this case $\alpha + \beta = k_3(1 + B/E) + k_5\mathrm{Cl}_{\Sigma}/(\mathrm{Cl}_{\Sigma} + k_5E/P)$ and $\alpha\beta = k_3k_5\mathrm{Cl}_{\Sigma}/(\mathrm{Cl}_{\Sigma} + k_5\ E/P)$ or $\alpha + \beta = \alpha\beta/k_3 + k_3(1 + B/E)$. If we introduce $R = \beta/\alpha$, this equation is expressed as a quadratic equation in k_3

$$R(1 + B/E)k_3^2 - \beta(1 + R)k_3 + \beta^2 = 0 \qquad (8)$$

which means that $\beta^2(1 + R)^2 - 4\beta^2R(1 + B/E) \geq 0$, which again implies that $(R - 0.05)(R - 17.95) \geq 0$, since B/E is approx. 4 [1].

Defining β as the smallest rate coefficient of Eqn. 6, it means that $\beta/\alpha \leq 0.05$. We have found that the small variations of $(1 + \beta/\alpha)$ with β has only negligeable effects when one of the measured β values (2% BSA and $V_{\Theta} = 500$) is used to estimate a κ value defined as $1/k_3 + (1 + B/E)/k_5$. The equation used to calculate β is, therefore,

$$\beta = \frac{T/y_{\infty}}{\frac{E + B}{P\mathrm{Cl}_{\Sigma}} + \frac{T/y_{\infty} + 4}{5}\kappa} \qquad (7.1)$$

when $AV_{\Theta} >> E + B$ then $T \approx y_{\infty}$ and

$$\beta = \frac{1}{\frac{E + B}{P\mathrm{Cl}_{\Sigma}} + \kappa} \qquad (7.2)$$

Results

The efflux rate coefficient (β) from ghosts to BSA

The data presented in Fig. 2 panel A and B are obtained in efflux experiments with $\nu = 0.7$ and $V_{\Theta} = 80$. For each of the three [BSA] 0.02%, 0.2% and 2%, we have done three or four efflux experiments. Firstly, the figure shows the reproducibility of efflux recordings; secondly, that the slope beyond 1.5 s (β) increases with the [BSA] and thirdly, that the slope is constant until the recorded 95% of the equilibrium value at 2% [BSA], whereas in the case of 0.2%, the slope becomes

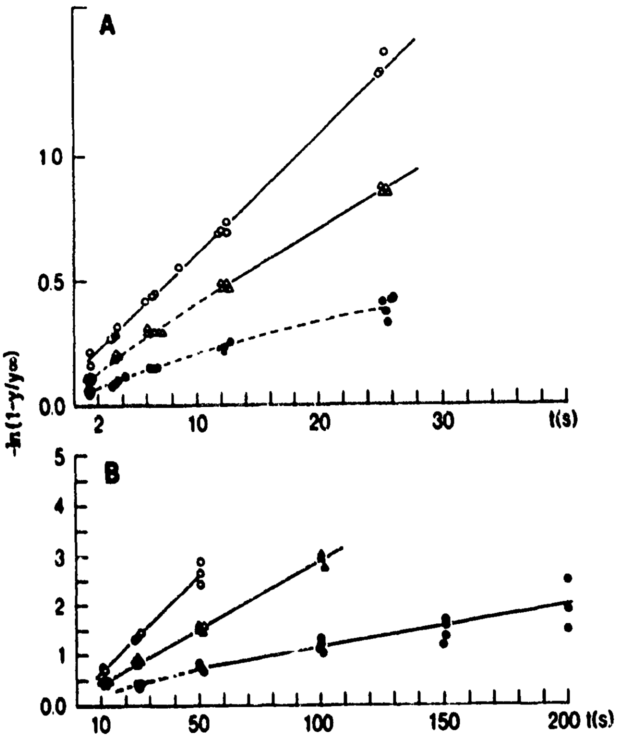

Fig. 2. Exchange efflux kinetics of [^{3}H]palmitate from ghosts at 0°C (pH 7.3) ν 0.7 into the extracellular medium. The ghosts were prepared in 165 mM KCl and the extracellular medium is 165 mM KCl, 2 mM phosphate buffer containing BSA and 0.02 mM EDTA/EGTA (1 : 1). ○, [BSA] 2%; △; [BSA] 0.2%; ●, [BSA] 0.02%. y is the amount of [^{3}H]palmitate in the medium at the time of sampling and y_∞ is the isotopic equilibrium value. (A) Data on the early part of the efflux from 1 to 30 s. (B) Data on the late part of the efflux from 10 to 200 s. The full-drawn lines are the linear regressions lines through the final data points defining the rate coefficient β.

constant only after 12 s (40% of equilibrium). This effect is even more pronounced for 0.02% [BSA] where the constancy is obtained after 50 s (53% of equilibrium) until the recorded 86% of the equilibrium value. Recording before 1.5 s is impossible, therefore, the 2%-curve appears to be monoexponential. However, the two other curves are compatible with the expected biphasic time-course in agreement with Eqn. 6. The ordinate intercepts of the three final slopes are about the same corresponding to a y/y_∞ of 0.2. Thus, we are able to evaluate the smallest rate coefficient signified by β in Eqn. 6.

When V_Θ is 500 and 80, y_∞ is virtually equal to T and the β value then is the rate coefficient of the slowly released PA, only a little smaller than the unidirectional PA released from the major fraction of ghost PA (80%), situated on the membrane inner surface [1].

ν is without significant effects on β

The amount of PA bound to ghost strongly depends on ν [7], therefore, we have investigated whether ν has any effect on β. Table I shows that β is virtually independent of ν although ν is varied from 0.15 to 0.94, corresponding to an about 10-fold increase in membrane bound PA [7]. Only in two cases are the differences statistically significant between the β values corresponding to two different ν values. However, the effects of ν are in opposite directions and may arise by chance in cases when the number of data in one of the groups are small.

TABLE I

The relationship between [BSA] and rate coefficient β at two different molar ratios (ν values) of PA to BSA at three different efflux volumes (V_Θ values)

Efflux experiments are carried out in 165 mM KCl, 2 mM phosphate buffer (pH 7.3) at 0°C. β values are estimated by linear regression (full-drawn lines in Fig. 2). The number of determinations is given in parentheses

[BSA] (%)	ν_1	$\beta_1 \pm$ S.D. (×1000) (s^{-1})	ν_2	$\beta_2 \pm$ S.D. (×1000) (s^{-1})
V_Θ = 500 (ml/ml ghosts)				
2	0.67	49.3 ± 2.3 (5)	0.15	49.8 ± 2.0 (4)
1	0.72	44.0 ± 1.0 (4)	0.15	44.0 ± 1.3 (4)
0.2	0.67	25.5 ± 1.3 (3) ^{a}	0.17	29.0 ± 2.0 (8) ^{a}
0.05	0.72	14.4 ± 1.1 (4)	0.17	15.5 ± 1.4 (8)
0.01	0.72	8.0 ± 1.2 (4)	0.15	8.7 ± 1.2 (4)
V_Θ = 80 (ml/ml ghosts)				
2	0.67	50.3 ± 3.5 (3)	0.21	50.1 ± 1.3 (2)
0.2	0.67	28.1 ± 2.1 (4)	0.21	26.6 ± 0.8 (7)
0.05	0.70	16.0 ± 3.8 (4)	0.21	15.9 ± 1.0 (3)
0.01	0.70	7.3 ± 0.6 (3)	0.21	7.6 ± 1.1 (4)
V_Θ = 36 (ml/ml ghosts)				
2	0.94	49.7 ± 1.5 (5) ^{b}	0.24	46.0 ± 0.4 (2) ^{b}
0.2	0.94	29.8 ± 1.7 (4)	0.23	27.3 ± 2.5 (3)
0.02	0.94	6.0 ± 2.6 (4)	0.23	8.8 ± 0.6 (3)

The differences ($\beta_1 - \beta_2$) are not significant, except in the cases marked ^{a} and ^{b}, where $P < 0.05$ and 0.02, respectively.

Thus, the rate of efflux is proportional to the membrane binding no matter whether the [BSA] is high or low and independent of a more than 10-fold variation of the ghost concentration.

The effect of [BSA] on the rate coefficient β with various V_Θ. Since β is independent of ν we have pooled all β values measured with different ν values. Table II presents mean β values measured at three V_Θ (500, 80 and 36) and six [BSA] (ranging from 0.01% to 2%). Statistical analyses reveal significant V_Θ effects only with [BSA] below 0.2%. This is demonstrated clearly in a double-log plot of the mean values of β vs. [BSA] (Fig. 3). Thus, we have been able to demonstrate that although a 10-fold increase of [BSA] from 0.2 to 2% results in a nearly 2-fold higher β, a 14-fold increase of medium volume (i.e., increasing the total amount of BSA) has no effect on β.

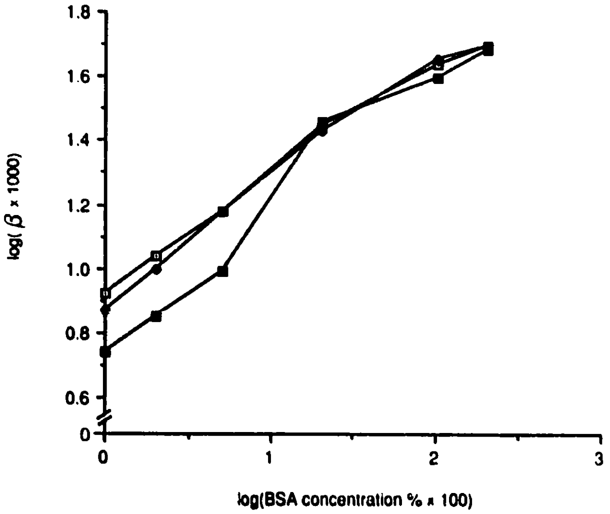

Fig. 3. A double-logarithmic plot of the efflux rate coefficient β (see Eqn. 6, Theory) vs. [BSA] of the efflux medium at various volumes of the medium (V_Θ) in ml/ml ghosts. ⊡, V_Θ-500 (ml/ml ghosts); ◆, V_Θ-80 (ml/ml ghosts) and ■, V_Θ-36 (ml/ml ghosts).

However, when the [BSA] is 0.05% or below, there are small significant effects of an increased V_Θ. An explanation is presented below.

Our data presented as in reports on cellular uptake of fatty acids. The equilibrium membrane binding of PA increases strongly with ν in the range 0.2 to 1.4 [7] and the rate of unidirectional PA release and binding is, therefore, proportional to the amount of PA bound in ghosts at any particular ν. We have measured this rate of release in exchange efflux experiments. In such experiments, the uptake and efflux are identical, therefore, we are able to present our data as 'uptake' rate,which is the amount of PA of the membrane inner surface (0.8 × B nmol, see Fig. 1 in Ref. 7) multiplied by the rate coefficient β s^{-1}.

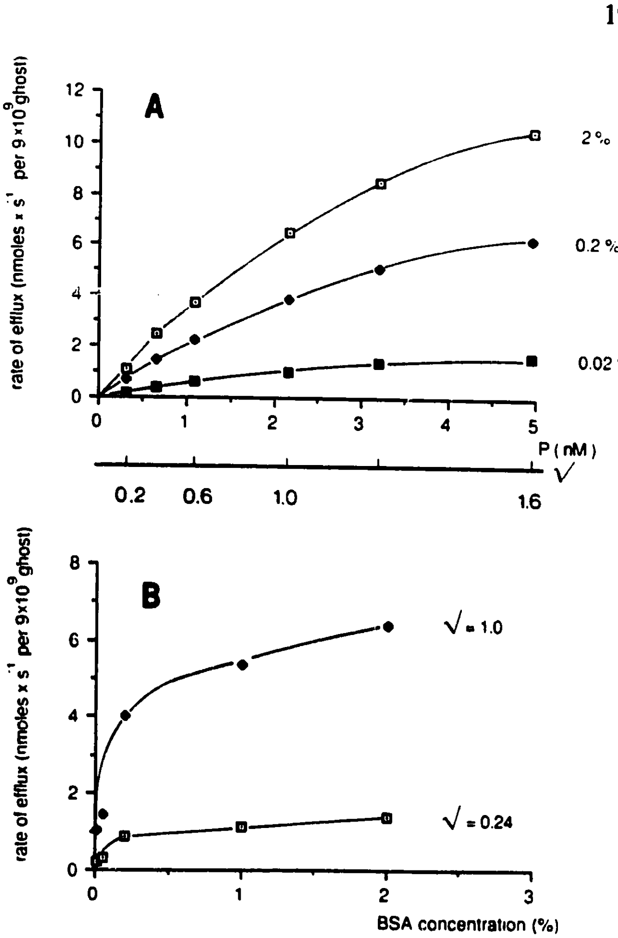

Fig. 4. Rate of unidirectional efflux from the inner surface binding capacity of the ghost membrane (A) vs. P, the unbound equilibrium palmitate concentration calculated as $\nu/(K_u\,(3-\nu))$ (see notations) at three different [BSA]. (B) vs. [BSA] at two different ν values.

Fig. 4A shows such 'uptake' vs. P, the equilibrium concentration of unbound PA and Fig. 4B shows 'uptake' as a function of [BSA] at two different ν values. However, the question on the net uptake-dependency of P and [BSA] by non-equilibrated cells is beyond the scope of the present paper.

TABLE II

The effects of BSA concentrations and medium to ghost ratios (V_Θ values) on the minor rate coefficient of palmitate exchange efflux, signified by β of Eqn. 6

S.E. signifies standard error of the mean and C.V. is the coefficient of variation (S.D./$\bar{X}$). The number of determinations is given in parentheses

[BSA] (%)	V_Θ = 500 (ml/ml ghosts)		V_Θ = 80 (ml/ml ghost)		V_Θ = 36 (ml/ml ghosts)	
	β ± S.E. (× 1000)	C.V.	β ± S.E. (× 1000)	C.V.	β ± S.E. (× 1000)	C.V.
2	49.5 ± 0.7 (9)	0.042	50.2 ± 1.2 (5)	0.05	48.5 ± 0.9 (7)	0.05
1	44.0 ± 0.4 (8)	0.026	46.0 ± 1.0 (2)	0.03	40.0 ± 1.2 (3)	0.06
0.2	28.1 ± 0.8 (11)	0.094	27.0 ± 0.4 (11)	0.05	28.7 ± 0.9 (7)	0.08
0.05	15.2 ± 0.4 (12)	0.082	15.5 ± 1.0 (7) [a]	0.14	9.7 ± 1.4 (3)	0.25
0.02	11.0 ± 0.5 (3)	0.076	10.1 ± 0.2 (4) [b]	0.04	7.1 ± 0.7 (7)	0.25
0.01	8.3 ± 0.4 (8) [d]	0.120	7.4 ± 0.2 (7) [c]	0.07	5.5 ± 0.7 (4)	0.24

[a] Differs from the corresponding β at $V_\Theta = 36$, $P < 0.001$.

[b] Differs from the corresponding β at $V_\Theta = 36$, $P < 0.01$.

[c] Differs from the corresponding β at $V_\Theta = 36$, $P < 0.01$.

[d] Differs from the corresponding β at $V_\Theta = 80$, $P < 0.05$.

Interpretation of the experimental data

The ν independency of β

The ν-dependent variables in the simplified Eqn. 7.1 are all comprised in the term: $(E+B)/(P\,\mathrm{Cl}_{\Sigma})$. Cl_u is by far the major variable part of Cl_{Σ}, since there is no effect of medium to ghost volume ratio (V_{Θ}) on β when [BSA] $\geq 0.2\%$ and only a small effect when [BSA] is below 0.2% (Table I, Fig. 3). The ν-dependency of P is described by the equilibrium constant (K_a) of the PA-BSA binding ($P = \nu/(K_a(3-\nu))$).

$\mathrm{Cl}_u = k_u S((1-e^{-\lambda\delta})/\lambda) = (k_1 A/P)S((1-e^{-\lambda\delta})/\lambda)$ where $\lambda = \sqrt{(k_1 A/P)/D}$ This expression can be simplified because $(1-e^{-\lambda\delta})$ is nearly 1 when [BSA] is 1% and 2% and depends otherwise very little on ν, at most about 10%.

Thus, we can reduce the expression of Cl_u to $S\sqrt{D}\sqrt{k_1 A/P}$, which gives $(E+B)/P\mathrm{Cl}_{\Sigma}$, which is approx. $(E+B)/P\mathrm{Cl}_u$, which is approx. $C(E+B)\sqrt{(3-\nu)}/(\nu\sqrt{k_1})$ where C contains only ν-independent factors. This shows that β is ν-independent if $(E+B)\sqrt{(3-\nu)}/(\nu\sqrt{k_1})$ is ν-independent. In a previous work [1], we have published the ν-dependency of k_1 and $(E+B)$, the latter expressed as Q, the ratio of membrane bound PA to PA on BSA (0.2%) in a volume corresponding to the ghost volume.

Using our mean values of the two parameters k_1 and Q for ν 0.2, 0.6 and 1.4 [1], we get the values 8.6, 9.7 and 11.0 for $(E+B)\sqrt{(3-\nu)}/(\nu\sqrt{k_1})$. The values 9.7 and 11.0 are hardly significantly higher than 8.7 with $P < 0.1$ and 0.05, respectively, whereas $\sqrt{(3-\nu)}/\nu$ decreases 9-fold from ν 0.2 to ν 1.4. We conclude that the observed ν-independency of β corroborates with our previous measurements.

The observed variations of β with [BSA] and medium to ghost volume ratio (V_{Θ})

In order to use Eqn. 7.1, we must again use our previously determined k_1 and Q values [1]. We have recently developed a new method [7] for the determination of the equilibrium constant (K_a) of PA binding to BSA and obtained the value $2.3 \cdot 10^8$ M^{-1} calculated with three hypothetical equivalent binding sites in the relevant range of ν. It is however, important to note that we use K_a in this work only to evaluate the ratio of albumin bound PA to the water phase monomer PA concentration at any ν value.

The diffusion coefficient D of monomer PA, which is the state in water of PA in equilibrium with BSA bound PA [7], is taken from the work of Patil et al. [26]. The value $7.2 \cdot 10^{-6}$ $\mathrm{cm^2\,s^{-1}}$ determined at 25°C is transformed into 360 $\mu\mathrm{m^2\,s^{-1}}$ at 0°C on basis of the temperature-dependency of water viscosity. The value corresponds to that of monomer laurate, since the directly measured diffusion coefficient of PA is claimed to be too low because of dimerization. A variation of ± 10% in D has no effect on the fitting value of V_u.

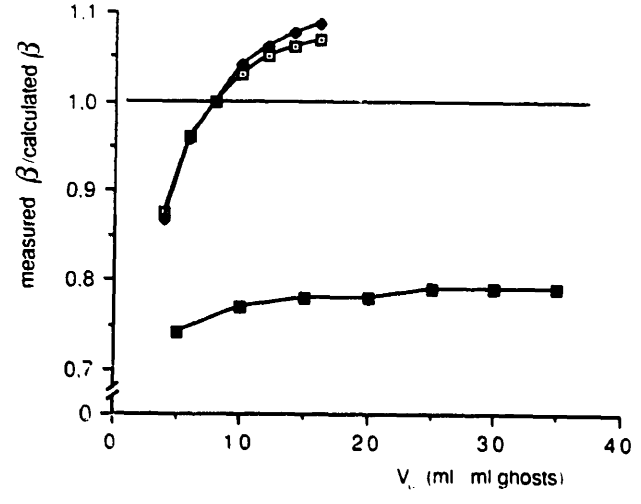

Fig. 5. The effect of provisional values of unstirred volume V_u (in ml/ml ghosts) on the weighted ratio of measured rate coefficient β to β calculated (Eqn. 7.1 (see Theory) with a fixed κ evaluated from $\beta = 0.0495$ (Tables I and II). To calculate β values, we use the parameters $D = 360$ $\mu\mathrm{m^2\,s^{-1}}$, $K_a = 2.3\times10^8$ $\mathrm{M^{-1}}$, $\nu = 0.6$, $k_1 = 0.0027$ $\mathrm{s^{-1}}$ and membrane bound PA $(B+E) = 7.74$ nmol/ml ghosts. ■, calculations according to spherical geometry of the unstirred volume (V_u) for all three medium/ghost volumes V_{Θ} (500, 80 and 36). ⊡, calculations according to planar geometry of the unstirred volume (V_u) for all V_{Θ} (500, 80 and 36); ◆, for V_{Θ} 80 and 500 only. Each point represents 17 and 11 determinations, respectively.

We have no possibility to assign definite values to the two rate constants of κ in Eqn. 7.1. We know, however, that k_3 must be much smaller than k_5 and, therefore, we can replace $(1+E/(V_{\Theta}A))/k_3 + (1+B/E)/k_5$ by $(1+E/(V_{\Theta}A))(1/k_3 + (1+B/E)/k_5)$ particularly since $E/(V_{\Theta}A)$ usually is negligible compared to 1, never exceeding 0.05.

In order to evaluate κ for any presumed value of V_u, we use the β value measured with 2% BSA and V_{Θ} 500 (Table II). On basis of this value of κ we get calculated β values corresponding to the remaining 17 measured β values. We neglect the difference between 1 and $(1+\beta/\alpha)$, since β/α never exceeds 0.055 (see above).

Fig. 5 shows the relation between provisional values of V_u and the mean of the 17 ratios of measured to calculated β weighted by the S.E. of the measured values. The mean ratio becomes 1 for V_u equal to 8 ml/ml ghost, which means that an USL of depth 6.2 μm may account for all the data. The S.E. of this mean ratio is 0.040, only a little higher than the minimum S.E. 0.037 obtained for V_u equal to 10 ml/ml ghost corresponding to a depth of 7.7 μm. Fig. 5 shows also that we get the same result by using only the data of $V_{\Theta} = 80$ and $V_{\Theta} = 500$. The special stirring technique used with $V_{\Theta} = 36$ has, therefore, not been important.

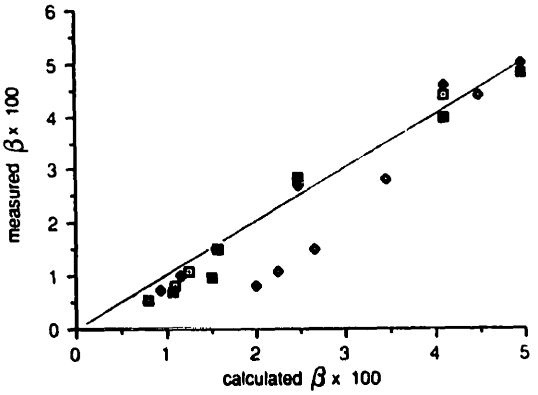

Fig. 6. The relationship between measured β values and calculated β values for unstirred volume $V_u = 8$ ml/ml ghost and planar geometry. The measured β corresponding to [BSA] = 2% and $V_{\Theta} = 500$ is used to get the parameter κ. Other parameters are listed in the legend to Fig. 5. ⊡, $V_{\Theta} = 500$ ml/ml ghost and increasing [BSA] 0.01, 0.02, 0.05, 0.2 and 1%; ◆, $V_{\Theta} = 80$ ml/ml ghost and [BSA] 0.01, 0.02, 0.05, 0.2, 1 and 2%; ■, $V_{\Theta} = 36$ ml/ml ghost and [BSA] 0.01, 0.02, 0.05, 0.2, 1 and 2%; ◇, β is calculated on basis of spherical geometry, $V_{\Theta} = 500$ ml/ml ghost and [BSA] 0.01, 0.02, 0.05, 0.2 and 1%.

Fig. 6 is a plot of measured β vs. calculated β for V_u 8 ml/ml ghost. It shows that the distribution around the line of identity is not random, but that the β values for small [BSA] (below 0.2%) are calculated somewhat too high, whereas the values corresponding to 0.2% and 1% are calculated too low. However, the main pattern of the data are obviously reproduced by the calculated β values. The calculated β is independent of the medium to ghost volume ratio, V_{Θ}, when [BSA] $\geq 0.2\%$, but decreases with $V_{\Theta} < 80$ when [BSA] $<$ 0.05%, corresponding to low β values.

Discussion

The efflux kinetics (Fig. 2) are compatible with the predicted time course expressed by Eqn. 6 and the smallest rate coefficient β is experimentally well-defined under a variety of conditions (Table I and II). Noteworthy is also that the β values obtained in the present experiments with 0.2% BSA agree very well with the mean β value of 0.0287 reported previously [1]. We, therefore, believe that our interpretation of the β variations in terms of the theoretical determinants (Eqn. 7.1) provide reliable information on the interactions of the determinants.

The result that β is independent of ν is unexpected because all the components of the variable term of Eqn. 7.2 ($(E+B)/(P\mathrm{Cl}_{\Sigma})$) are ν-dependent. However, close analysis shows that the variations of the components with ν balance fairly well. This means that the present data validate the previous results which are obtained by different kinds of experiments. Particularly interesting is the ν effect on the dissociation rate constant of PA-BSA complex (k_1) within the low range of ν from 0.2 to 1.4. It can only be understood as a kinetic cooperativity of occupied binding sites which may be hard to accept in this low ν range. However, it is readily calculated in the way used by Spector and Fletcher [28] that at ν 0.2 and 0.6 and three equivalent binding sites 12 and 32%, respectively, of the ligand molecule is bound with two binding sites occupied on the same albumin molecule.

The β-independence of ν has also direct implications of interest

Considering the two diagrams of Fig. 4 as diagrams of unidirectional uptake (binding of PA by ghosts), they remind of the diagrams made on basis of data obtained in shortlasting incubations of cells in buffer with albumin bound fatty acids [13–17].

On basis of such diagrams it has been claimed that fatty-acid uptake exhibits 'saturation kinetics' and that albumin binding may be a rate-determining process [13–17]. Both interpretations are, however, invalid. According to the present analyses neither of the two independent variables are directly rate-determining parameters. The 'saturation kinetics' reflects the properties of USL and tells nothing about the membrane transport.

Why an USL must be invoked

Provided the volume surrounding the ghosts is homogeneous with regard to tracer water-phase concentration, i.e., perfectly stirred, increased binding capacity must have the same effect whether it is produced by an increased [BSA] in a constant volume or by an increased volume with constant [BSA]. Therefore, increasing the medium to ghost volume ratio (V_{Θ}) from 36 to 360 is expected to be equivalent to an augmentation of [BSA] from say 0.2 to 2%. However, Fig. 4A demonstrates unequivocally that this is not the case and that BSA of a limited volume is of major importance. In other words, that an USL exists, in which the transport occurs solely by diffusion. Furthermore, if we use Eqn. 7.1 under the assumption that the whole medium is stirred efficiently, the calculated β values are grossly inconsistent with the measured β values. In the case of no USL we have $\mathrm{Cl}_{\Sigma} = k_1 V_{\Theta} A/P$. If we, for instance, consider V_{Θ} 36 and use the highest β 0.05 to estimate κ, then the five remaining calculated β values are all much higher, in average 2-fold higher than the measured β values although they decrease with [BSA]. A somewhat better fit is obtained by using a k_1 value four fold smaller than the known value [1]. A similar poor fit of calculated β with V_{Θ} 500 requires a further 6-fold reduction of k_1. Thus, we are unable to account for the data if we assume that the medium is homogeneous, as regards reactant concentrations, whereas we understand the pattern by assuming that 8 ml medium per ml ghost is unstirred, independently of the actual V_Θ, which varied from 36 to 500.

It is, furthermore, important to note the difference between the two interpretations (1) of Fig. 4, diagram B according to Eqn. 7.1 and (2) by assuming no USL. In the latter case, we only need a little more than 2% BSA to get the maximum transport rate at any ν value, whereas there is no limit of the effect of increasing [BSA] according to Eqn. 7.1. Since κ is about 9 with V_u 8 ml, the maximum of β is not about 0.05 but 0.11 reached with 'infinitely high' [BSA].

The origin and size of USL of suspended cells

Investigations of the membrane transport of solutes, such as oxygen and chloride with high membrane-permeability require experiments with suspended cells and evaluation of the significance of USL and/or techniques to minimize the size of USL to insignificant values. The question has, therefore, been dicussed for many years [29] and it has been possible to reduce the depth of USL surrounding red cells and probably also ghosts to 1–2 μm by using a fast continuous-flow system with a high degree of turbulence [19]. With a stop-flow arrangement, the depth is, however, extended considerably to 5–6 μm, probably because the turbulence decays rapidly [20]. Unfortunately, we have not found any experimental incubation system directly relevant to ours, but the theoretical work of Rice [19] on USL of cells in systems with quasilaminar flow is relevant and instructive. Accordingly, the most important determinant is the velocity gradients in the medium when the cells and the medium do not have very different densities. Important is also the diffusion coefficient of the solute in question, since the depth of USL is inversely proportional to the cubic root of the diffusion coefficient [19]. USL has no precise depth but it is defined by the distance from the surface where the solute transport changes from the diffusion dominated to a convectional dominated process. This aspect of USL has in fact been suggested many years ago [29]. Although it is known that the geometry of the unstirred volume around suspended cells must be important for the effect on transports, the question has not been solved [19].

The depth of USL of a suspended cell is always calculated from the effects of a plane sheet with area of the cell, even in the work of Sha'afi et al. [20]. The depth of a shell (δ') surrounding a sphere with radius r is related to the depth of a sheet (δ) covering the same area and with the same volume as the shell by

$$\delta'/r = \left(\sqrt[3]{3\cdot\delta/r}\right) - 1$$

Thus, our δ value of 6 μm covering a plane area as large as the surface area of a ghost with r 3 μm corresponds to a δ' of 2.45 μm. However, the diffusion resistance of the plane sheet 6 μm thick is 4.5-fold greater. This is readily calculated from the expressions of the two resistances $\delta/(4\pi r^2 D)$ and $\delta'/(4\pi r(r+\delta')D)$ for the sheet and the shell, respectively. The depth of a sheet with the same resistance as a shell with δ' 2.45 μm is 1.3 μm and not 6 μm.

Also, the equation accounting for the supply of monomer from the membrane surface by diffusion to BSA in a shell is very different from that of plane sheets. It has been developed as outlined by Bass and Pond [30]. Using this equation together with the equation of the diffusion resistance of a shell, we are able to calculate the β values for various values of V_u as described before. As shown from the results presented in Fig. 5, no value of V_u makes in average the calculated β values fit the measured β values. The calculated β values corresponding to [BSA] 0.2% and smaller are much too high particularly with high V_Θ. The failure of the shell equations to account for the observations arises from the low diffusion resistance of a shell which has the sufficient depth. We conclude that the USL is not a shell but functions much like a plane sheet for reasons not known so far. The possibility remains to be investigated that the diffusion in USL occurs essentially in two dimensions, i.e., an oblate geometry surrounding ghosts.

The agreement of calculated with measured β values makes it interesting to analyze the changes in the tracer uptake by BSA in V_u and V_s in relation to changes in BSA concentrations and V_Θ according to the theory. Table III shows the contributions of the two terms, Cl_u and $1/(1/Cl_s + R_D)$ to the total clearance Cl_V.

It can be seen that Cl_u decreases greatly with [BSA] in contrast to the almost constancy of $1/(1/Cl_s + R_D)$. This result can be understood by the model. According to the theory $Cl_u = S\sqrt{k_u}\sqrt{D}(1 - e^{-\lambda\delta})$, since $\lambda = \sqrt{(k_1 A/P)/D} = \sqrt{k_u/D}$. k_u depends on the [BSA], as it is equal to $K_u k_1$ [BSA] $(3 - \nu)$, therefore, when

TABLE III

Theoretical analysis of the tracer uptake by bovine serum albumin (BSA) in unstirred volume (V_u) and stirred volume (V_s)

[BSA] (%)	$(V_s' + V_u')$ (ml/ml ghosts)	Cl_u [a] (ml s^{-1})	$1/(1/Cl_s + R_D)$ [a] (ml s^{-1})
2	36	516	77
	500	516	77
0.2	36	142	74
	500	142	77
0.02	36	20	52
	500	21	75

[a] Cl_u and $1/(1/Cl_s + R_D)$ are calculated using $D = 360$ $\mu m^2 s^{-1}$, $k_1 = 0.0027$ s^{-1}, $\delta = 6$ μm, $\nu = 0.6$ and for the calculation of k_a and P, $K_a = 2.3\cdot10^8$ M^{-1}.

[BSA] decreases, Cl_u decreases with the square root of [BSA] as long as $e^{-\lambda\delta} \ll 1$, but else much more, since $\lambda\delta$ decreases with the square root of [BSA].

In the term $1/(1/\mathrm{Cl}_s + R_D)$, $\mathrm{Cl}_s = V_s k_a$, Cl_s must decrease with [BSA] along with k_a. However, at [BSA] 2%, it can be seen that an increase of V_Θ (an increase of V_s) has apparently no consequence for the term $1/(1/\mathrm{Cl}_s + R_D)$. The reason is that $1/\mathrm{Cl}_s$ is negligible compared to R_D and the term $1/(1/\mathrm{Cl}_s + R_D)$ is equal to $1/R_D = 77.5$, which sets the limit of the contribution of V_s. In other words, above a certain lower limit an increasing conductivity in series with a resistance has no effect on the current. In our case this limit is set by a k_a corresponding to [BSA] 0.2% and V_Θ 36 ($V_s = 28$) and/or a k_a corresponding to [BSA] 0.02% and V_Θ 500 ($V_s = 492$).

Our result with regard to USL is in many ways comparable to the results of Sha'afi et al. [20], except for the use of ghosts instead of red cells. The systems are similar in that there is no turbulence of the suspensions under the measurements. Furthermore, both investigations deal with low molecular weight solutes, so that differences in diffusion coefficients plays no significant role, including the effect of different temperatures (20°C and 0°C). Also the ranges of cell concentrations are similar. Finally, both calculations of the depth of USL are based upon the geometry of a plane sheet with the same area as that of the cell. It is, therefore, gratifying that the results are almost identical, although they are obtained with so very different 'detection methods'.

In conclusion: The ghosts are in well stirred suspensions surrounded by an USL, which has the effects of a plane sheet, 6 μm deep and with the same area as a ghost. It causes a dependency on ν and [BSA] of the unidirectional efflux rates of PA bound at the inside of the membrane, which is similar to the FA uptake by a variety of cells investigated by others. Our findings question the validity of any inference about membrane transport kinetics which neglect the USL effects. Saturation kinetics may elude any unequivocal demonstration, but a membrane binding capacity has in fact already been shown by other means to mediate the translocation of PA across the ghost membrane [1].

The diffusion resistance of even a narrow, 6 μm, USL is critical for the PA transport rate along such a distance because of low monomer concentration levels. Albumin within USL reduces the resistance and this makes the albumin concentration a critical determinant of the transport.

Appendix

The distribution of BSA-bound tracer

In the Theory section, this is assumed to be virtually uniform in the entire medium. The assumption makes it possible to describe the processes in terms of a compartmental model, which fits the data fairly well (Figs. 2 and 6). The major binding occurs within the unstirred volume V_u, particularly when [BSA] $\geq$ 0.2% (Table III) and it is important to understand why the bound PA is not accumulated within V_u to such extent that the specific activity of bound tracer has a larger effect than expected of a uniform distribution. The USL of BSA and, thus, of bound tracer, is smaller than USL of PA by the cubic root of the diffusion coefficient ratio ($\sqrt[3]{D_{BSA}/D_{PA}}$, [19]), and therefore, about 3 μm, since the diffusion coefficient of BSA at 0°C is about 32 $\mu m^2 s^{-1}$. This value has been obtained by transformation on basis of the temperature-dependency of water viscosity of the value 5.9×10^{-7} $cm^2 s^{-1}$ determined by Wagner and Scheraga [31] at 20°C. The unstirred volume of BSA (V_{BSA}) is correspondingly about 4 ml/ml ghost. The binding rate is exponential decreasing through V_u and a major fraction of the binding in V_u occurs within V_{BSA} if [BSA] is 2%. If we can account for a virtual uniform distribution of bound tracer exclusively formed within V_{BSA}, the same must be true also within V_u.

The argument uses two basic equations:

$$\mathrm{I}: \; dy/dt = \beta(y_\infty - y)$$

$$\mathrm{II}: \; -(dQ/Q)/dt = (\pi^2 D/(4\delta^2)),\; Q = (V_{BSA}(a_u - a_s))$$

Eqn. I is obtained simply from the definition of β within the slow-efflux phase ($\beta = d(-\ln(1 - y/y_\infty))/dt$). Eqn. II is a differential expression of the equation derived by Jacobs (Eqn. 40 in Ref. 22) to describe the kind of processes in question. The equation is simplified by using only the first exponential term. It describes the rate by which an amount Q of a solute with the diffusion coefficient D decreases by diffusion from the mean concentration a_u in a layer with the thickness δ, volume V_{BSA}, through one open boundary to a stirred larger volume with the concentration a_s. The rate constant of Eqn. II ($\pi^2 D/(4\delta^2)$) is in our case very large (9 s^{-1}). The rate constant of Eqn. I is $\beta(y_\infty/y - 1)$ at most 0.2 s^{-1}, since the highest values of β and y_∞/y of the slow phase are 0.05 and 5, respectively. The much higher rate constant of escape from V_{BSA} than of formation is in harmony with the basic assumption of quasistationary states within V_{BSA}. We can then express the ratio of mean concentration within V_{BSA} to mean concentration within the entire medium at any y_∞/y state by

$$\mathrm{III}: \; a_u/a = (1/20)(19 + y_\infty \mathrm{Cl}_{s}/y)$$

This equation is obtained as follows: Since $y = a_u \cdot V_{BSA} + a_s \cdot V_s$, the concentration a_s in Eqn. II can be substituted by $(y - a_u V_{BSA})/V_s$ and by using the values for D and δ given above we get Eqn. II as $-dQ/dt = 9V_{BSA}/V_s(a_u \cdot V_\Theta - y)$ or $-dQ/dt = (a_u \cdot V_\Theta - y)$, since V_{BSA}/V_s is about 1/9.

A quasistationary state (input = output) is then expressed by

$$\beta(y_\infty - y) = a_u \cdot V_\Theta - y$$

with $\beta = 0.05$ and $y/V_\Theta = a$, we get Eqn. III.

Calculation of a_u/a values according to Eqn. III for different y/y_∞ values gives: a_u/a: 1.45, 1.2, 1.05 and 1 for y/y_∞ 0.1, 0.2, 0.5 and 1, respectively. The deviation from uniform distribution of bound tracer when the rate of binding is great is, however, as shown below unimportant, because of the very low specific activity of bound tracer compared with that of the monomer.

The level of y/y_∞ at which the specific activity of bound tracer begins to have an effect on the efflux can be estimated as follows.

By using the assumption that Cl_s is approx. Cl_u, Eqn. 5 tells us that if $\text{Cl}_u Py/(V_\Theta A) \ll dy/dt$, then the bound tracer plays no role for the rate of efflux. As shown above, $dy/dt = \beta(y_\infty - y)$ and the bound tracer plays no role at the levels of y_∞/y of which the inequality holds true: $(\text{Cl}_u P/(AV_\Theta))/(\beta(y_\infty/y - 1)) \ll 1$.

Using $\beta = 0.05$, $V_\Theta = 36$, $\nu = 0.6$ and the other parameters given in legend to Fig. 5, we get 0.002 and 0.02 for the left-hand side of the inequality when y_∞/y is 2 and 1.1, respectively.

In conclusion: the effect of the bound tracer on the efflux is negligeable for $y_\infty/y > 2$ ($y/y_\infty < 0.5$) and the slight accumulation of bound tracer within V_u calculated above as maximum values are entirely insignificant.

Acknowledgements

We want to thank Irene Jørgensen for skilfull technical assistance. The work was supported by grant 11-8978 from The Danish Natural Science Research Council and by grant from the NOVO-Foundation, Copenhagen, Denmark.

References

1 Bojesen, I.N. and Bojesen, E. (1991) Biochim. Biophys. Acta 1064, 297–307.
2 Brodersen, R., Honore, B. and Andersen, S. (1988) Eur. J. Biochem. 174, 45–50.
3 Brodersen, R., Vorum, H., Skriver E. and Pedersen, A.O. (1989) Eur. J. Biochem. 182, 19–25.
4 Weisiger, R.A., Gollan, J. and Ockner, R. (1981) Science 248, 1048–1051.
5 Weisiger, R.A., Pond, S.M. and Bass, L. (1989) Am. J. Physiol. 257, G904-G916.
6 Funder, J. and Wieth, J.O. (1967) Acta Physiol. Scand. 71, 105–112.
7 Bojesen, I.N. and Bojesen, E. (1992) J. Lipid Res. 33, 1327–1334.
8 Spector, A.A., John, K. and Fletcher, J.E. (1969) J. Lipid Res. 10, 56–67.
9 Spector, A.A., Fletcher, J.E. and Ashbrook, J.D. (1971) Biochemistry 10, 3229–3232.
10 Goodman, DeW.S. (1958) J. Amer. Chem. Soc. 80, 3887–3892.
11 Spector, A.A. (1975) J. Lipid Res. 16, 165–178.
12 Storch, J. and Kleinfeld, A.M. (1986) Biochemistry 25, 1717–1726.
13 Abumrad, N.A., Park, J.H. and Park, C.R. (1984) J. Biol. Chem. 259, 8945–8953.
14 Sorrentino, D., Robinson, R.B., Kiang, C.-L. and Berk, P. (1989) J. Clin. Invest. 84, 1325–1333.
15 Stremmel, W., Stromeyer, G. and Berk, P.D. (1986) Proc. Natl. Acad. Sci. USA 83, 3584–3588.
16 Sorrentino, D., Stump, D., Potter, B.J., Robinson, R.B., White, R. Kiang, C-L. and Berk, P.D. (1988) J. Clin. Invest. 82, 928–935.
17 Stremmel, W. (1989) Mol. Cell. Biochem. 88, 23–29.
18 Spector, A.A., Ashbrook, J.D. Santos, E.C. and Fletcher, J.E. (1972) J. Lipid Res. 13, 445–451.
19 Rice, S.A. (1980) Biophys. J. 29, 65–77.
20 Sha'afi, R.I., Rich, G.T. Sidel, V.W., Bossert, W. and Solomon, A.K. (1967) J. Gen. Phys. 50, 1377–1399.
21 Brahm, J. (1983) J. Gen. Phys. 81, 283–304.
22 Jacobs, M.H. (1967) Diffusion Processes, Springer, Berlin.
23 Chen, R.F. (1967) J. Biol. Chem. 242, 173–181.
24 Bojesen, I.N. (1985) Prostaglandins 30, 479–489.
25 Armitage, P. (1971) Statistical Methods in Medical Research, Blackwell, Oxford.
26 Patil, G.S., Matthews, R.H. and Cornwell, D.G. (1973) J. Lipid Res. 14, 26–31.
27 Crank, J. (1964) in The Mathematics of Diffusion, Clarendon, Oxford.
28 Spector, A.A. and Fletcher, J.E. (1978) in Disturbances in Lipid and Lipoprotein Metabolism (Dietschy, J.M., Gotto, A.M., Jr. and Ontho, J.A., eds.), pp. 229–249, American Physiology Society, Bethesda, MD, USA.
29 Barry, P.H. and Diamond, J.M. (1984) Physiol. Rev. 64, 763–872.
30 Bass, L. and Pond, S.M. (1988) in Pharmacokinetics: Mathematical and statistical approaches to metabolism and distribution of chemicals and drugs. (Pecile, A. and Rescigno, A., eds.) pp. 245–269, Plenum, London.
31 Wagner, M.L. and Scheraga, H.A. (1956) J. Phys. Chem. 60, 1066.